ISSN 2635-1676, Nanobiotechnology Reports, 2024, Vol. 19, No. 3, pp. 393–407. © Pleiades Publishing, Ltd., 2024.
Russian Text © The Author(s), 2024, published in Rossiiskie Nanotekhnologii, 2024, Vol. 19, No. 4, pp. 505–519.

NANOBIOLOGY AND GENETICS, OMICS TECHNOLOGIES

# Comparative Metagenomics for Monitoring the Hidden Dynamics of the Algal-Bacterial Wastewater Community under the Influence of Drugs

**P. A. Zaytsev[a,*], B. M. Shurygin[a], V. A. Rodin[a], T. V. Panova[a], M. I. Zvereva[a], E. V. Skripnikova[b], and A. E. Solovchenko[a]**

[a] *Moscow State University, Moscow, 119991 Russia*
[b] *Belgorod National Research University, Belgorod, 308015 Russia*
**E-mail: zaytsevpa@my.msu.ru*

Received March 2, 2024; revised April 19, 2024; accepted July 9, 2024

**Abstract**—Modern methods of metagenomics, including those based on long reads of nanopore sequencing, are especially relevant for environmental-monitoring tasks, in particular, for assessing the anthropogenic impact on natural communities of microorganisms. These include algal-bacterial communities that live in water-treatment plants and participate in the biological treatment of wastewater from excess organic waste and nutrients (phosphorus and nitrogen). Metagenomic analysis shows changes in the taxonomic composition and functional profile of the algal-bacterial community when simulating the release of drugs into wastewater: broad-spectrum antibiotics (for example, ceftriaxone) and nonsteroidal anti-inflammatory drugs (for example, diclofenac). The results of metagenomic analysis based on long reads of nanopore sequencing and classical methods of environmental monitoring, including metabarcoding based on short reads on a second-generation sequencing platform, are compared. Nanopore sequencing of the entire metagenome shows a greater biodiversity of samples compared to the DNA metabarcoding of short reads, makes it possible to determine the taxonomic affiliation of particular organisms more accurately, identify groups of eukaryotic oxygenic phototrophs, and also reveal the presence of antibiotic-resistance genes in the community. It is shown that under the influence of medicinal substances, the algal-bacterial community is enriched with antibiotic-resistant bacteria. At the same time, despite maintaining the rate of phosphorus removal, the community's potential for the removal of nutrients is reduced, which is expressed in a two-order reduction in the relative representation of inorganic-nutrient metabolism genes. Simultaneous exposure to ceftriaxone and excess nutrients in the wastewater leads to the maximum enrichment of antibiotic-resistant organisms, as well as the replacement of cyanobacteria originally present in the community with eukaryotic microalga.

**DOI:** 10.1134/S2635167624600470

## INTRODUCTION

Municipal and industrial wastewater in water-treatment plants (WTPs) even after a three-stage wastewater-treatment system may contain organic waste and inorganic compounds with biogenic properties (bioavailable inorganic forms of nitrogen and phosphorus) that exceed the maximum permissible concentrations (MPCs) which may induce eutrophication of water bodies when released into the environment. In addition, other specific classes of micropollutants, such as medicinal compounds, i.e., antibiotics, lipid-lowering medications, anti-inflammatory drugs, β-blockers, mood-stabilizing agents, increase the anthropogenic load [1, 2].

The availability of natural light and substrates for growth triggers the formation of algal-bacterial communities (ABCs) in WTPs, in which oxygenic-phototrophic microorganisms (OPMs), i.e., eukaryotic green microalgae and cyanobacteria, act as edificators [3]. It is known that OPMs in ABCs in activated sludge are capable of reducing the macronutrient concentration in wastewater due to their biomediated removal [4–6], as well as the biodegradation of harmful micropollutants [7–9]. The role of the bacterial component in an ABC may be associated with the promotion of OPM growth by MGP bacteria (microalgal-growth-promoting bacteria) [10, 11] as these bacteria produce cofactors and vitamins [12, 13] or enhance macronutrient bioavailability (nitrogen and phosphorus) [14]. Furthermore, the bacteria of ABCs may absorb macronutrients from wastewater, including via the enhanced biological phosphorus removal (EBPR) mechanism or anaerobic ammonium oxidation (anammox), i.e., processes that were proven to occur in ABCs in [15, 16]. To increase the stability and efficiency of ABCs in wastewater treatment, it is important to develop tools for analyzing and monitoring

these systems, including based on the multiomics approach that employs metagenomic analysis [17–20]. Metagenomics is the use of DNA-sequencing techniques to investigate the genetic diversity of species and represents a powerful tool for studying the microbial world. Metagenomics is a popular approach in environmental assessment, the investigation of environmental disasters, and the search for strains of microorganisms for ecological remediation [21, 22].

A major advantage of metagenomics is that it is a culture-independent method and it enables the researcher to study the hidden microbial diversity from uncultivated microbial samples, which is especially relevant for algal-bacterial communities that change under anthropogenic impact. Since metagenomics does not provide comprehensive information about the physiological state of an ABC and the processes occurring in it, the metagenomic approach needs to be combined with other methods of environmental monitoring, such as microscopy, functional monitoring of the photosynthetic apparatus, analysis of the chemical composition of the environment, and others.

The classic metagenomics methods, such as DNA metabarcoding and complete metagenome sequencing by next-generation sequencing (NGS), have a limited DNA read length, which leads to coarse taxonomic resolution in metabarcoding and the incomplete assembly of metagenomes [23]. In addition, in contrast to analysis of the complete metagenome, metabarcoding does not allow the researchers to suggest the physiological and metabolic potential of the sample. Indirect predictions in terms of these issues may be inferred using the PICRUSt2 and Tax4Fun2 algorithms [24, 25], but their accuracy is far from ideal.

In recent years, third-generation sequencing has been progressing rapidly, which includes nanopore sequencing [26]. This was made successfully commercially available by the Oxford Nanopore Technologies (ONT). Nanopore sequencing enables generation of long-read sequences (100000 bases and longer) and the sequencing of single molecules without measuring the average signal in a group of molecules. It also means DNA may be sequenced directly without sequencing DNA intermediates, which reduces the risk of systematic error because of selective enrichment at specific parts of the genome and/or certain microorganisms [21, 27]. Although nanopore sequencing was initially less accurate than other sequencing technologies, modern sample-preparation protocols and algorithms of data analysis have reduced the error rate to an acceptable 0–5% [28, 29]. Nanopore sequencing offers real-time rapid insight into samples and on-demand sequencing, thus enabling analysis even in field conditions [27, 30].

Whole metagenome sequencing is the gold standard for metagenomic studies of different community samples as it makes it possible to generate large amounts of sequence data that enables researchers to comprehensively analyze communities. Metagenomics offers the accurate taxonomic identification of eukaryotic and prokaryotic species in communities, confirms the presence or absence of functionally significant genes, enables the search for new effective and stable enzymes, as well as metabolic-model reconstruction directly from metagenomes [31–33]. The technologies and methods used in metagenomics allow the direct analysis of raw sequence reads: phylotyping of organisms based on the direct counting of their genetic markers from raw sequencing reads without alignment [34, 35], more accurate taxonomic identification using BLAST, MEGAN, or TAXAssign [35–37], or profiling of species-level genome bins using the MetaPhlan computational tool [38]. Although these approaches to processing metagenomic data are focused on prokaryotes, new algorithms are being developed for eukaryotic microorganisms, including for the microalgae of ABCs [39, 40]. The analysis of raw sequence reads may also be used to detect functionally significant genes in the search for certain metabolic pathways, such as the degradation of harmful micropollutants, i.e., genes of polyethylene terephthalate hydrolase (PETase) and mono–2-hydroxyethyl terephthalate hydrolase (MHETase) involved in plastic degradation [40]; genes of chromium reductase and genes responsible for the bioaccumulation of iron and manganese in the phycoremediation of heavy metals [41, 42]; nitrilase genes in xenobiotic degradation and others [43–47]. For the rapid analysis of ABCs in environmental monitoring, the significant factors are free availability and fast analysis provided by a gradually increasing number of online platforms such as BugSeq and MGnify [47, 48]. The long-read direct analysis of raw nanopore sequence reads is faster and more accurate compared with metagenome assembly using short reads [47].

The purpose of this work is to study the evident and hidden changes in the structure and properties of the ABC microbiome when exposed to drugs, including antibiotics (using ceftriaxone, a common antibiotic, and a group of cephalosporins as an example) and nonsteroidal anti–inflammatory drugs (diclofenac as an example). Furthermore, we compare the observed changes in the morphophysiological properties of ABCs with changes in their metagenomes revealed by the reference method of NGS-metabarcoding and nanopore sequencing.

## MATERIALS AND METHODS

*Samples of communities and cultivation conditions.* The samples of ABCs from activated sludge and wastewater were collected at the Municipal Water Supply Service of Zvenigorod in June 2021. Samples were taken from wastewater-filled secondary settling

**Table 1.** Composition of wastewater*

| Parameter | Units of measurement | Value | MPC |
|---|---|---|---|
| Hydrogen indicator | units of pH | 7.54 ± 0.20 | 6.5–8.5 |
| Ammonium nitrogen | mg of N/L | 0.29 ± 0.07 | 0.40 |
| Nitrite ion | mg of N/L | <0.06 | 0.08 |
| Nitrate ion | mg of $NO_3^-$/L | 30.02 | 40.0 |
| Phosphate ion | mg of $PO_4^{3-}$/L | 15.25–1.53 | 0.05–0.15 |
| Anionic surface-active agents | mg/L | 0.404 ± 0.129 | 0.5 |
| Chloride ion | mg of $Cl^-$/L | 114.60–11.46 | 300.0 |
| Sulphate ion | mg $SO_4^{2-}$/L | 55.21–5.52 | 100 |
| Petroleum products | mg/L | 0.005 ± 0.03 | 0.05 |
| Total iron | mg/L | 0.136 ± 0.049 | 0.10 |
| Suspended substance | mg/L | 144.2 ± 17.3 | +0.75 to the background concentration |
| Dichromate oxidation (Chemical oxygen demand, COD) | mg of $O_2$/L | 17.6–5.3 | 5.0 |

*According to the data obtained at the Accredited Analytical Laboratory "Certification Center and Ecological Monitoring of the Moskovskii Agrochemical Agency".

tanks into a common clean nonsterile container. Wastewater was collected at WTPs after tertiary treatment: after post-treatment, but before the disinfection stage. Experiments with activated sludge and wastewater (Table 1) were performed on the day of sample collection.

To model the stress associated with the effect of drugs on the ABC of activated sludge upon standard and elevated concentrations of inorganic phosphate ($P_i$) for wastewater, cultivation was carried out under steady-state conditions similar to those in the secondary settling tanks. Cultivation was carried out in 75 mL sterile plastic culture vials (Eppendorf, Germany) with a filter under illumination by LED lamps (white light, 5500 K) with an intensity of 50 μmol of PAR/$m^2$/s (measured with an LI250 light sensor, LiCOR, United States), at room temperature for 31 days. A total of 5 mL of raw biomass of ABC from activated sludge was added to each vial and brought to 40 mL with wastewater. Solutions of ceftriaxone (**CTA**, Biosynthesis LLC, Russia) or diclofenac (**DF**, Chemopharm A.D., Serbia) were added to the sludge beds, and in some variants supplementary sources of phosphorus and nitrogen were added ($K_2HPO_4$ and $KNO_3$) (Table 2). As a control of the drug effect, the ABC biomass of wastewater was used without the addition of drugs, but it contained the supplementary sources of phosphorus and nitrogen. Wastewater without biomass and additives was used as the control in metagenomic analysis. Each experimental variant was incubated in triplicate.

During the experiment, the state of the photosynthetic apparatus of the OPMs from the studied communities was monitored by analyzing chlorophyll-*a*-fluorescence induction curves. At the end of incubation, biomass samples were taken for the extraction of metagenomic DNA and morphological analysis by optical microscopy, and culture liquid samples were used to determine the residual content of $P_i$ by spectrophotometry using molybdenum blue [49].

*Extraction of metagenomic DNA*. To isolate the total DNA for each experimental variant, biomass samples (0.3–0.5 mL) were collected. Before the start of extraction, the cell sediments were frozen in liquid nitrogen and ground to a fine powder using homogenization pestles (SSIBio, United States) in a 1.5-mL microcentrifuge tube. The freeze–homogenization procedure was performed trice. The total DNA from the samples was extracted using the DNeasy Plant Pro Kit (QIAGEN, Germany) as recommended by the manufacturer.

*Nanopore sequencing of samples and bioinformatic analysis of the results*. The nanopore sequencing of

**Table 2.** Design of experiment

| Experimental variant | Additives (final concentration, mg/L) |
|---|---|
| Wastewater | |
| +P+N | $K_2HPO_4$ (50), $KNO_3$ (100) |
| +CTA | CTA (5) |
| +DF | DF (5) |
| +P+N+CTA | $K_2HPO_4$ (50), $KNO_3$ (100), CTA (5) |
| +P+N+DF | $K_2HPO_4$ (50), $KNO_3$ (100), DF (5) |

samples was performed according to the Oxford Nanopore Technologies (ONT, United Kingdom) genomic DNA sequencing technology using the Native barcoding genomic DNA protocol (SQK-LSK109) and the MinION sequencer (ONT, United Kingdom) using an R9.4.1 flow cell (ONT, United Kingdom). The first stage included DNA repair and preparation of the ends for the ligation of barcodes and adapters using the NEBNext Companion Module for Oxford Nanopore Technologies Ligation Sequencing E7180S (New England Biolabs, United States). DNA was purified using Agencourt AMPure XP magnetic beads (Beckman Coulter, United States). At the second stage, unique barcodes from the Native barcoding Expansion 1–12 kit (EXP-NBD104, ONT) were added, and the ligation reaction was run using the Blunt/TA Ligase Master Mix (New England Biolabs). Barcoding reagents with numbers 3–8 were used. DNA purification using the Agencourt AMPure XP magnetic beads (Beckman Coulter, United States) was repeated. After purification, barcode amplicons were mixed in equimolar proportions. At the third stage, adapters from the SQK-LSK 109 kit (ONT, United Kingdom) were ligated using the Quick T4 DNA Ligase (New England Biolabs). DNA cleanup steps were performed using Agencourt AMPure XP magnetic beads (Beckman Coulter), the samples were washed with buffer to bind long DNA fragments, and the elution step was performed using a buffer from the SQK-LSK 109 kit (ONT, United Kingdom) resulting in a ready-to-use DNA library. At the last stage, the library was prepared for the start of sequencing using the SQK-LSK 109 kit (ONT, United Kingdom) and the constructed libraries were loaded into the R9.4.1 flow cell (ONT). The flow cell was placed in the sequencer and the sequencing process was initiated. As the dataset was accumulated, sequencing was discontinued. The flow cell was washed with Flow Cell Wash reagents (ONT, United Kingdom). The primary nanopore-sequencing data were written into FAST5 files and converted into FASTQ format. The primary raw data were converted using Guppy basecaller software (ONT). The samples were debarcoded using Guppy basecaller software during the raw-data post-processing. The $Q < 8$ read accuracy datasets of Guppy basecaller were discarded from subsequent analysis.

For bioinformatic analysis of the data, all FASTQ output files from the directory of the astq_pass files were merged into one file with the same format for each sample. The generated reads were analyzed with the BugSeq online bioinformatics platform (https://bugseq.com) using the NCBI nt database and the sample type "environmental."

*Profiling of the taxonomic composition of communities by the 16S rRNA locus*. The microbiome composition was analyzed by DNA metabarcoding based on the hypervariable V4 region of the 16S rRNA gene using primers F515 and R806 (GTGCCAGCMGCCGCGGTAA and GGACTACVSGGGTATCTAAT) [50] with the Illumina MiSeq system. The libraries were prepared as recommended by the MiSeq Reagent Kit Preparation Guide (Illumina, United States). For this, PCR was run as follows: 94°C, 30 s; 55°C, 30 s; 72°C, 30 s; 25 cycles, primary denaturation at 94°C for 60 s; the final stage of elongation was run for 3 min at a temperature of 72°C. The PCR products were purified as recommended by Illumina using AMPureXP (Beckman Coulter, United States).

The libraries were sequenced with a generation of pair-end reads (2 × 300 bp run). The primary sequences were processed using Illumina software. Subsequent processing steps, in particular, sequence merging into ASV (Amplicon sequence variant), were carried out using the software packages: dada2 [51], phyloseq [52], and DECIPHER [53]. Taxonomic profiling was performed using QIIME tools [54]. The SSU 16s rRNA SILVA database, release 132 [55], was used as the reference-sequence database.

During the analysis of DNA metabarcoding datasets, unclassified reads, plastid and mitochondrial DNA reads, as well as the taxonomic groups with one unpaired read, were removed from the samples. During analysis, biological replicates were combined for each experimental variant, and the read numbers for all ASVs were summed. For the obtained datasets corresponding to the biological replicates of the experiment, the mean values of the read numbers for all ASVs were calculated. The Shannon–Weaver (1) and Simpson (2) diversity indices, as well as the Morisita β-diversity index (3) were calculated using the formulas [56]:

$$H = \sum_{i=1}^{N} \left(-p_i \ln\left(p_i\right)\right), \quad (1)$$

$$D = \sum_{i=1}^{N} p_i^2, \quad (2)$$

where $p_i$ is the proportion of short reads corresponding to taxon $i$ of the total number of short reads for the sample, $N$ is the total number of taxa in the sample;

$$\chi_{ij} = \frac{2\sum_{k=1}^{S}\left(n_k^i n_k^j\right)}{\left(\frac{\sum_{k=1}^{S}\left(n_k^i\right)^2}{\left(N^i\right)^2} + \frac{\sum_{k=1}^{S}\left(n_k^j\right)^2}{\left(N^j\right)^2}\right) N^i N^j}, \quad (3)$$

where $N_i$ and $N_j$ are the total number of taxa in samples $i$ and $j$, respectively, $S$ is the number of taxa common for samples $i$ and $j$, and $n_{ki}$ and $n_{kj}$ are the number of short reads that correspond to the common taxa $k$ in samples $i$ and $j$, respectively.

The Morisita β-diversity index was also used for the pairwise comparison of taxonomic datasets obtained based on metabarcoding and sequencing

data of the complete metagenome on the Oxford Nanopore platform. The values of the diversity indices were visualized using an algorithm in the Python programming language (version 3.7.1) using the Matplotlib library.

Functional annotation of the metabarcoding results was performed using the PICRUSt2 algorithm for taxonomic profiles at the level of genera without additional options [24].

*Determination of the inorganic phosphate concentration*. To determine the residual concentration of $P_i$ in the medium, a reagent containing 1.2 g of ammonium paramolybdate ($(NH_4)_6Mo_7O_{24}$; Sigma Aldrich, United States), 12 g of potassium antimonyl tartrate ($K_2Sb_2(C_4H_2O_6)_2$; Sigma Aldrich, United States), 32 mL of dilute sulfuric acid (concentrated sulfuric acid : bidistilled water = 1 : 1), bidistilled water (up to 100 L) was prepared according to the method [49]. The measurement was carried out in a 96-well transparent flat bottom plate (Eppendorf, Germany). A total of 200 μL of culture liquid containing $P_i$, 8 μL of ammonium paramolybdate reagent, 2 μL of 7.2% (weight : volume) ascorbic-acid solution ($C_6H_8O_6$; Sigma Aldrich, United States) was added to each well. Afterwards, the solution was incubated for 20 min at room temperature, and the optical density was recorded at λ = 880 nm using the Tecan Infinite M200 Pro plate spectrophotometer (Tecan, Switzerland). The $P_i$ concentration was calculated using the formula

$$C_{Pi} = \frac{3D_{880}}{0.13}, \quad (4)$$

where $C_{Pi}$ is the concentration $P_i$ in the medium (mg/L) and $D_{880}$ is the optical density at 880 nm.

*The state of the photosynthetic apparatus* was assessed by analyzing the induction curves of chlorophyll-*a* fluorescence using a FluorCam FC 800-C pulsed fluorimeter (Photon Systems Instruments, Czech Republic). The parameters for the OPMs were recorded directly in the culture beds after adapting the samples to the dark for 15 min. To record the curves, the manufacturer's NPQ protocol was used: a saturation flash intensity of 4000 μmol of PAR/$m^2$/s, the wavelength of the excitation light is 400–450 nm, detection at 620 nm, and the flash time is 2 s. During image processing, an area of interest was manually selected for each sample, from which the mean fluorescence value was obtained after the subtraction of background fluorescence. To assess the state of the photosynthetic apparatus of OPMs, the maximum quantum yield parameters of photosystem II (PSII) were calculated using the formula

$$Q_y = \frac{F_v}{F_m} = \frac{F_m - F_0}{F_m}, \quad (5)$$

where $Q_y$ is the maximum potential photochemical quantum yield of PSII, $F_0$ and $F_m$ are the minimal and maximal level of chlorophyll-*a* fluorescence after the saturation flash, respectively.

*Optical microscopy*. Morphological analysis of the ABCs was performed using bright-field microscopy on a Leica DM2500 (Leica Microsystems, Germany) equipped with a DFC 7000T camera (Leica Microsystems, Germany). Eukaryotic microalgal cells were visualized by recording the autofluorescence of chlorophyll *a*. To visualize the remaining cells in the ABCs, a solution of the fluorescent dye 4',6-diamidino-2-phenylindole (**DAPI**) dissolved in dimethyl sulfoxide at a concentration of 1 mg/mL was used. A total of 10 μL of the initial DAPI solution was added to 90 μL of the cell suspension and incubated for 20 min in the dark. Fluorescence images were obtained using the Leica DM2500 microscope (Leica Microsystems, Germany) with the Leica DFC700T camera. Fluorescence was excited by irradiation with an HXP 120 UV lamp (Leica Microsystems, Germany) equipped with a D filter (Leica Microsystems, Germany), in the range of 355–425 nm. Fluorescence emission was detected in the range of 455–700 nm. The appearance of ABCs in the culture beds was recorded using a digital camera.

## RESULTS AND DISCUSSION

*Appearance and morphology of the studied communities*. In laboratory conditions, stress was modeled for ABC activated sludge samples associated with the inclusion of medicinal substances (CTA or DF) into wastewater at concentrations typical for wastewater of 5 μg/L. Herein, the samples were incubated with drugs and excess macronutrient concentrations for these wastewaters in order to assess the effect of the drugs on the ability of ABCs to remove biogenic elements. By the end of the experiment, the appearance and morphology of the ABCs incubated with various additives (Table 1) differed in different experimental variants (Fig. 1a). In the sample with only nitrogen and phosphorus added, moderate flocculation of the biomass with a characteristic blue-green color was observed, indicating the presence of cyanobacteria in the floccules. In all samples incubated with the addition of DF, biomass flocculation was more noticeable, and their color changed (Fig. 1a). In all samples incubated with the addition of CTA, a more homogeneous biomass with a characteristic green color for microalgae was observed.

Based on the results of optical microscopy, microalgae developed more strongly in ABCs when incubated with CTA than in other samples (Fig. 1b). This was confirmed by images in the mode of chlorophyll-*a*-fluorescence imaging (Fig. 1c). In the samples incubated with the addition of DF, similar to the control, the biomass mainly included filamentous cyanobacteria and bacterial aggregates (Fig. 1b).

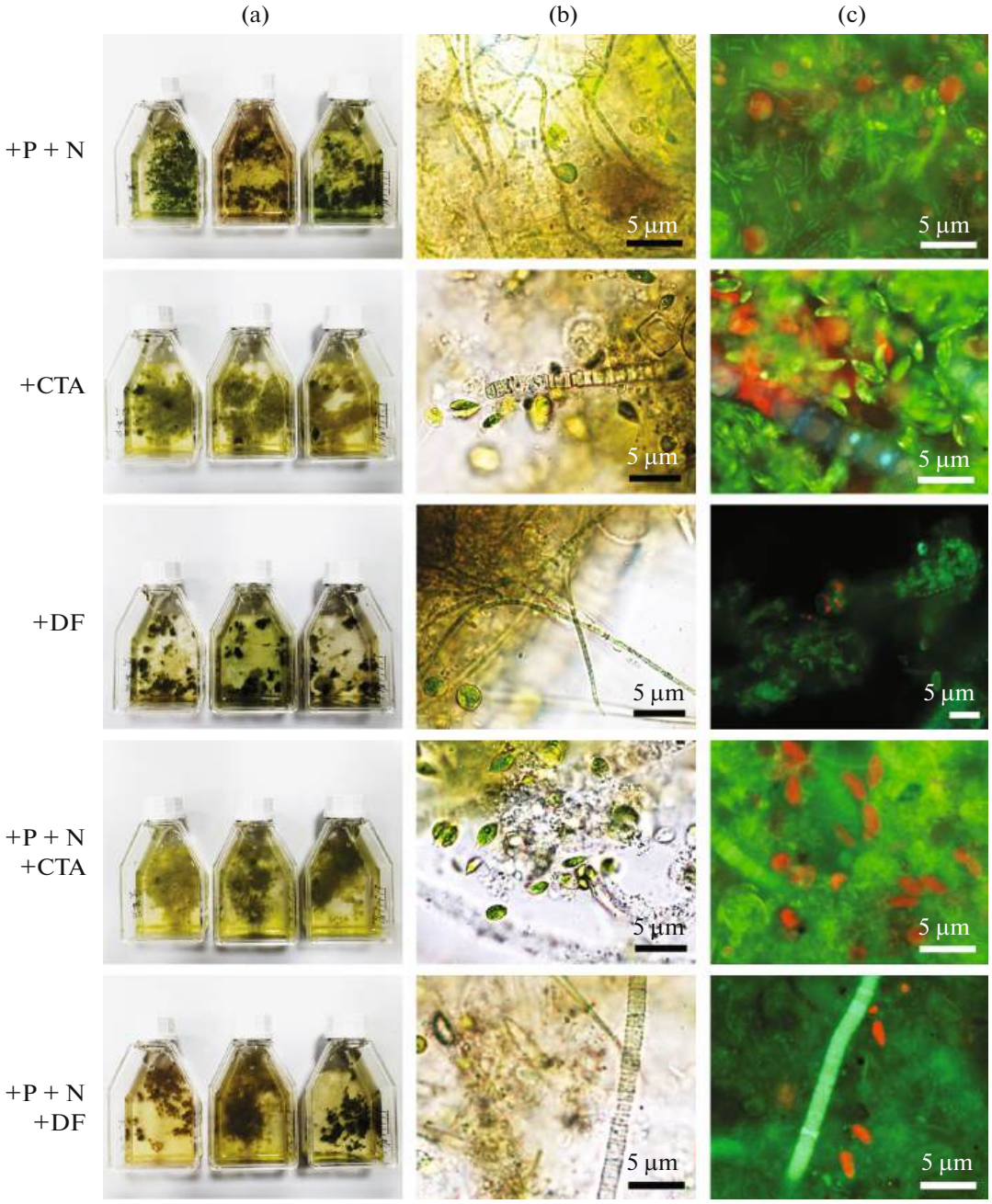


**Fig. 1.** Morphological features of the ABC samples from the Zvenigorod water-treatment plants after 31 days of incubation in wastewater with additives of drugs and/or nitrogen and phosphorus sources (Table 1): (a) the appearance of the ABC suspension, (b) transmission-electron-microscopy images of the ABCs, (c) fluorescence-microscopy images of ABC samples in the range of 455–700 nm.

*Dynamics of the state of the photosynthetic apparatus during incubation*. The physiological state of microalgae and cyanobacteria in the studied samples of ABCs was assessed by the functional parameters of their photosynthetic apparatus (Fig. 2). In all samples, a day after the start of incubation, the value of the maximum quantum yield of PSII, i.e., $Q_y$, increased slightly. This was probably due to acclimation to new, more favorable conditions (with better availability of nitrogen and phosphorus). Further, the $Q_y$ values decreased (in all samples as well) regardless of the additives. In the case of samples incubated without the addition of drugs, as well as samples with the addition of DF, the $Q_y$ value continued to decrease throughout the experiment to values in the range of 0.2–0.3. This may be explained by an increase in the cyanobacterial component in the ABCs.

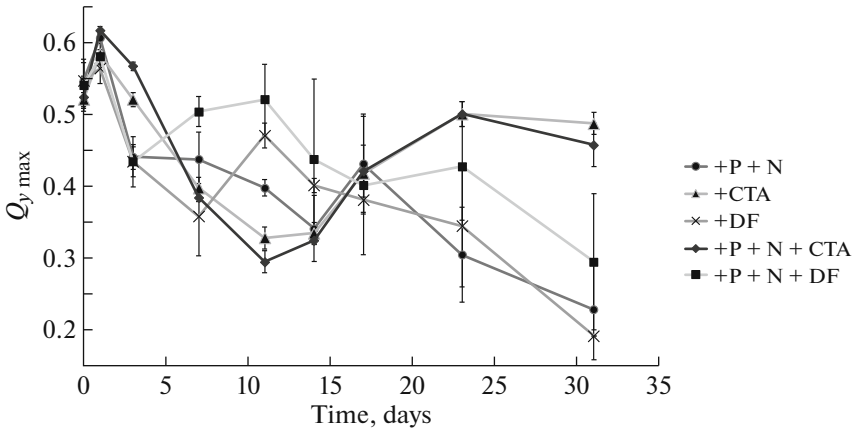


**Fig. 2.** Dynamics of the maximum potential photochemical quantum yield ($Q_y$ max) of photosystem II of the ABC samples from Zvenigorod water-treatment plants during incubation in wastewater with the addition of biogenic elements and/or drugs (Table 2). The graph shows the arithmetic mean values ($n = 6$) and the standard deviation.

During incubation of the samples with the addition of CTA, the $Q_y$ values decreased during the first 10 days, after which $Q_y$ increased again and reached a steady-state level of ~0.50. Thus, at least some photoautotrophic microorganisms in the composition of ABCs succeeded to adapt to the antibiotic action and became dominant in the community. Based on the values of $Q_y$, as well as the results of morphological analysis, the abundance of microalgae increased in the samples incubated with CTA.

Due to the absence of a significant difference between the dynamics of $Q_y$ values in the control sample (+P+N) and samples with DF, it is assumed that the different effects of the drugs on ABCs result from the development of one group of OPMs, i.e., microalgae upon the addition of CTA and cyanobacteria with the addition of DF, rather than being a consequence of direct action on PSII. Generally, the quantum yield of PSII in microalgae is higher than in cyanobacteria [57]. According to [45, 58], both cyanobacteria and microalgae are tolerant to CTA and DF in the concentrations used in the study and are able to reduce the activity of these compounds in solutions. However, a comparative analysis revealed that microalgae have higher growth rates upon the addition of CTA and cyanobacteria upon the addition of DF [59, 60]. The pattern of the $Q_y$ dynamics curve upon the addition of CTA was also consistent with the pattern obtained earlier using the microalgae *Lobosphaera* sp., in which $Q_y$ increased 10 days after adaptation [45].

*Bioremoval* of *inorganic phosphate by communities of microorganisms*. Upon completion of the incubation of ABCs with the studied drugs, the ability of communities to remove $P_i$ from wastewater was evaluated. The measurement of the residual $P_i$ content in the culture fluid samples showed that the communities consumed most of the $P_i$ initially contained in wastewater. In samples with a low initial $P_i$ content (5 mg/L), the bioremoval rate was 70%, and when the initial $P_i$ concentration was increased to 50 mg/L, it reached 95% (Fig. 3). In the case of a low initial concentration of $P_i$, the components of the community experienced stress due to a lack of bioavailable nitrogen, which weakened their ability to absorb $P_i$ [61]. It is noted that the sensitivity limit of the $P_i$ assay used in this work is 1 mg/L; therefore, the exact determination of the $P_i$ residual concentrations of ~1–2 mg/L (hence, the percentage of bioremoval) in cultures with a low $P_i$ content is a complicated task.

An important result is the lack of significant differences between the abilities to remove $P_i$ by ABC samples incubated with or without the addition of drugs. Apparently, the concentrations of drugs used in the work did not have a significant effect on phosphorus metabolism in the cells of microorganisms that form the basis of ABCs. It is also possible that microorganisms susceptible to the action of drugs were quickly replaced in the community by more tolerant components, while the integral indicator (absorption of $P_i$) remained at the level of ABCs that were not incubated with drugs.

*Effect of incubation with drugs on the microbiome structure*. Amplicon sequence data of the hypervariable fragment V4 of the 16S rRNA gene using the Illumina NGS sequencing platform were obtained for all the studied samples, with an average of 15 000 forward and reverse reads for each sample. For samples "wastewater", "+P+N", "+CTA", "+DF", "+P+N+CTA", and "+P+N+DF", the data in the FASTQ file for forward and reverse reads are available in the NCBI database under the BioProject number PRJNA1101684 and the BioSamples numbers SAMN40996167–SAMN40996172, respectively. Based on the data, the composition and relative quantity of microorganisms were determined (Fig. 4a). The

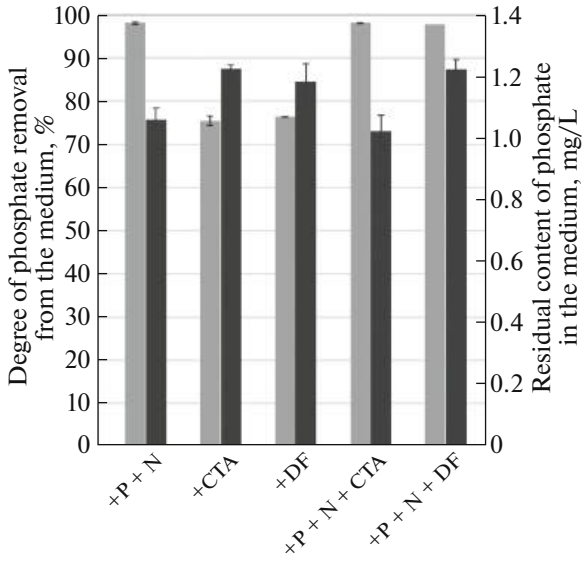


**Fig. 3.** Degree of phosphate removal from wastewater (light gray) and the residual phosphate content in the wastewater (dark gray) in the ABC samples from Zvenigorod water-treatment plants by the end of the month of incubation in wastewater with micropollutants.

taxonomic composition of the samples had many genera in common not only with each other, but also with the control sample of wastewater without the addition of biomass.

The following features are characteristic of ABCs: in samples incubated with drugs (+DF, +CTA), cyanobacteria of the *Limnothrix* genus were replaced by representatives of the *Leptolyngbya* and *Nodosilinea* genera; in the samples incubated without the addition of macronutrients, cyanobacteria of the *Leptolyngbya* genus developed; in the DF+N+P sample cyanobacteria of the *Leptolyngbya* genus were replaced by representatives of the *Nodosilinea* genus; bacteria from the *Alphaproteobacteria* class (the *Shingomonas*, *Brevundimonas,* and *Roseomonas* genera) were more abundant in the CTA samples, while cyanobacteria were less diverse (*Pseudanabaena* genus). In general, the *Cyanobacteria* class was more abundant in the samples with DF, but their content decreased during incubation of the community with CTA, which confirms the results of the morphophysiological features of the samples. Representatives of *Alphaproteobacteria* from the *Shingomonas*, *Brevundimonas,* and *Roseomonas* genera are known for their tolerance to different groups of antibiotics and other drugs, participate in their degradation in different systems, as well as include pathogenic species with an antibiotic-resistant phenotype [1, 2, 62]. It is noted that cyanobacteria of the *Leptolyngbya* genus develop in samples with drugs without additives of macronutrients (+DF, +CTA), which are characteristic of wastewater having a high level of organic and inorganic contamination [63]. It is possible that the addition of drugs to wastewater drives selection among microorganisms not only towards antibiotic resistance, but also in terms of general toxicological resistance to various micropollutants.

An assessment of the effect of incubation with drugs on the biodiversity of microbial ABC components showed that the drugs did not affect the Shannon–Weaver index, whose value fluctuated near 2.5 (Fig. 4b). At the same time, there was a slight decrease in the direct Simpson index from 2.0 to 1.5 in the CTA samples, which may indicate a shift in the community structure upon selective pressure caused by CTA. A pairwise assessment of the similarity between the microbiomes of the samples using the Morisita index revealed low similarity for all samples except those incubated with CTA, whose index was 0.57 (Fig. 4c). Thus, despite the similarity of the microbiome between the studied samples (some genera were found in each sample), individual drugs in concentrations comparable to those routinely detected in the environment and wastewater [5, 64] are able to change the abundance of taxa. At the same time, the addition of CTA causes similar changes in the microbiome, regardless of macronutrient availability.

*Analysis of the microbiome structure in communities using nanopore sequencing*. In nanopore sequencing, the following volumes of data were obtained for each sample: "wastewater," 0.22 GB; "+P+N," 0.53 GB; "+CTA," 0.39 GB; "+DF," 0.24 GB; "+P+N+CTA," 0.50 GB; "+P+N+DF," 0.43 GB. For the listed samples, data in FASTQ file are available in the NCBI database under the BioProject number PRJNA1101684 and the BioSamples numbers SAMN40996167–SAMN40996172, respectively.

The results of 16S gene metabarcoding were compared with the rapid sequencing of the complete metagenome using the same DNA samples by nanopore technology. The results of identification of the most represented genera of microorganisms in ABCs by the direct analysis of raw nanopore reads and NGS-metabarcoding coincided in many ways (Fig. 5a). However, due to direct calculation of the reads and absence of an amplification stage in preparation of the libraries, the quantitative distribution of microorganisms according to nanopore-sequencing data more accurately reflects the structure of ABCs. Thus, despite the common array of microorganisms in all ABCs, in samples with CTA and the addition of macronutrients, there is a gradual development of heterotrophic bacteria (from the *Shingomonas*, *Brevundimonas*, *Sphingomonas,* and *Tabrizicola* genera) and a decrease in the abundance of cyanobacteria (from the *Pseudanabaena* and *Leptolyngbya* genera).

The analysis of the reads obtained by sequencing the complete metagenome also made it possible to search for eukaryotic microalgae in samples of ABCs, the presence of which was difficult to confirm based on 16S gene metabarcoding data. It was found that the number of reads corresponding to representatives of

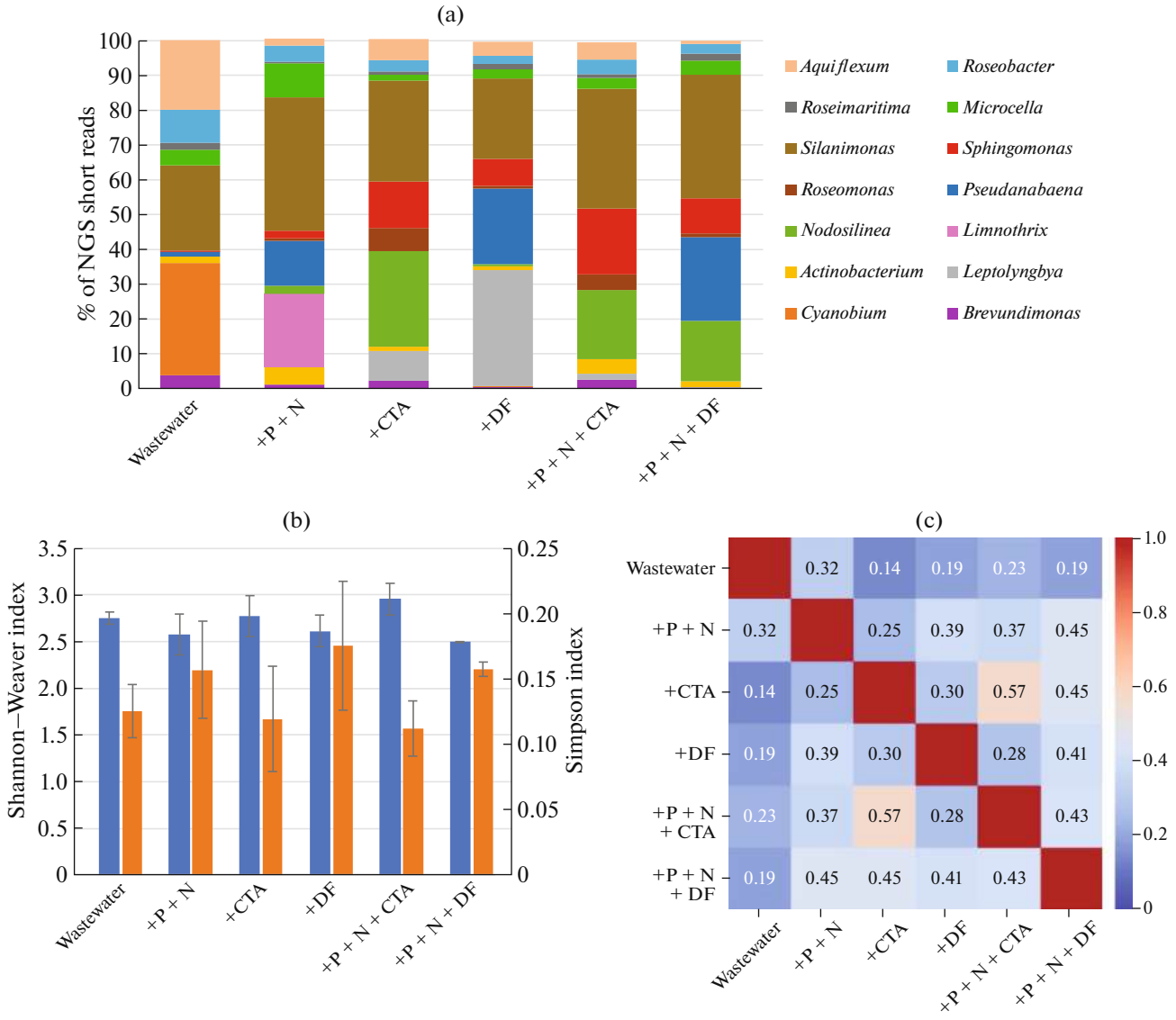


**Fig. 4.** Microbiome structure of the ABC samples from Zvenigorod water-treatment plants by the end of the month of incubation in wastewater with micropollutants described by 16S rRNA NGS metabarcoding: (a) the content of short reads of dominant microorganisms (>1%) in the microbiome at the level of genera, (b) calculated Shannon–Weaver α diversity (blue) and Simpson indices (orange), (c) a heat map of the values of the Morisita β-diversity index.

the *Chlorophyta* division (mainly the *Tetradesmus*, *Desmodesmus,* and *Chlorella* genera) was the highest in samples of biomass incubated with the addition of macronutrients, as well as macronutrients and CTA, and it ranged from 2 to 3% of the total number of reads. Meanwhile, cyanobacteria developed most strongly in the sample with macronutrients and DF, reaching 30% of the total number of reads (Fig. 5b). Although these results do not completely coincide with the data of traditional methods, they appear more solid, since calculations of raw reads are directly related to the ABC structure, in contrast to indirect estimates based on the general microscopy of complex structured samples (Fig. 1). Finally, the analysis of long reads from nanopore sequencing made it possible to classify microorganisms in ABCs with greater accuracy and identify such species as *Staphylococcus epidermis*, *S. haemolyticus*, etc., which are potential carriers of antibiotic resistance [65] that developed in the sample with the addition of macronutrients and CTA.

A quantitative comparison of the results obtained using two different platforms and sequencing generations was performed using metrics for evaluating diversity (Fig. 5b). Although it is not correct to apply these estimations for the analysis of raw reads during sequencing of the complete metagenome due to the lack of normalized genome length, they outline community differences. Thus, the values of the Shannon–

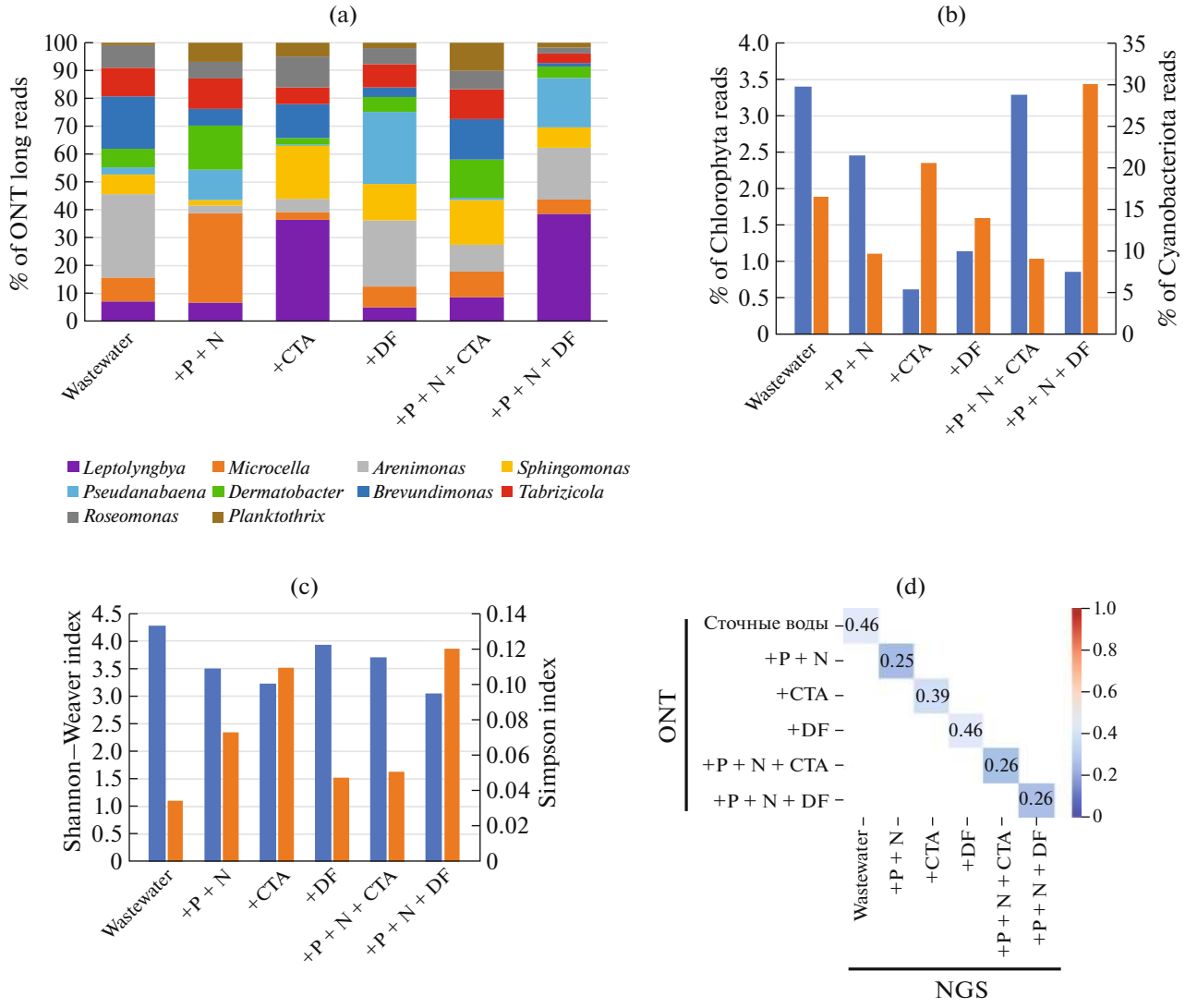


**Fig. 5.** Microbiome structure of the ABC samples from Zvenigorod water-treatment plants one month after incubation in wastewater with drugs (Table 1) obtained using the ONT nanopore sequencing method: (a) the content of long reads of the ten most represented microorganisms in the microbiome at the level of genera, (b) the content of OPMs in the microbiome at the level of the divisions *Chlorophyta* (blue) and *Cyanobacteriota* (orange), (c) calculated Shannon–Weaver α diversity (blue) and Simpson indices (orange), (d) a heat map of the values of the Morisita diversity index calculated for the results of nanopore sequencing (ONT) and 16S rRNA metabarcoding (NGS) for each sample.

Weaver index of all samples in nanopore sequencing exceeded the values in metabarcoding and ranged from 3.0 to 4.2, which may indicate an advantage of nanopore sequencing in studying the hidden microbial diversity of low abundant species in a community. This may be due to the fact that the direct classification of raw reads by their taxonomic affiliation lacks a stage of ASV or OTU (operational taxonomic unit) formation, which combines sequences of closely related organisms. Among the samples, the values of the Shannon–Weaver index for ABCs with the addition of CTA and DF+N+P were notable, which were lower than all others and amounted to 3.2 and 3.0, respectively. At the same time, the values of the direct Simpson index for the same samples were higher than the other samples, which is consistent with the metabarcoding results and indicates the active selection of microorganisms under these conditions. The pairwise similarity of samples between the two sequencing technologies was evaluated using the Morisita index calculated for the dominant genera (abundance >1%) (Fig. 5d). The results show no significant similarity between the sequencing methods for all samples, and the samples +N+P, DF+N+P, and CTA+N+P revealed the least similarity between the results of metabarcoding and nanopore sequencing, and the index was in the range of 0.25–0.26. Despite the different possible nature of

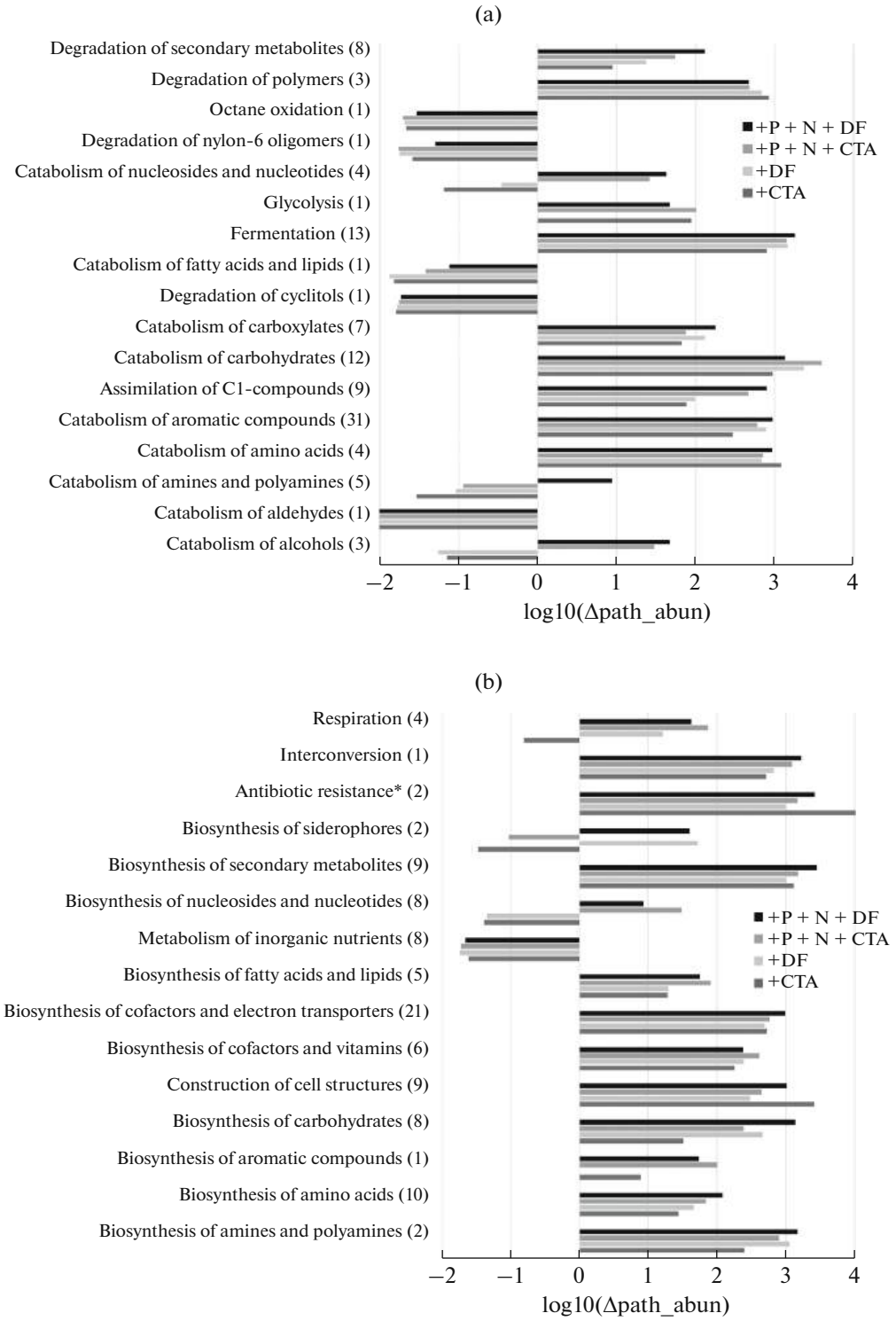


**Fig. 6.** Functional review of the representation of metabolic pathways in the ABC samples from Zvenigorod water-treatment plants after 31 days of incubation in wastewater with drugs: (a) pathways of substrate degradation, (b) pathways of biosynthesis. The number of pathways found for this superclass is shown in parentheses. (*It is assumed that antibiotic resistance is associated with induction of the biosynthesis pathway of bacterial cell-wall components).

such differences, they only emphasize the dependence of the metagenomic results on the choice of the sequencing method of a biological sample.

*Impact of drugs on the potential functional profile of the community*. Based on 16S rRNA metabarcoding data, a quantitative assessment of the potential repre-

sentation of genes encoding metabolic pathways at the superclass level was performed using the PICRUSt2 algorithm and the MetaCyc database classification [66]. Herein, it was predicted that a total of 201 metabolic pathways combined into 32 superclasses may be present in the studied ABCs (Fig. 6). This variety was divided into two parts: pathways involved in the degradation of substrates (Fig. 6a) and pathways responsible for the biosynthesis of various compounds (Fig. 6b). The representation of superclasses of metabolic pathways in ABC samples incubated with drugs was analyzed versus the samples incubated without the addition of drugs, but with supplementary macronutrients.

It was established that incubation with drugs reduced the representation of genes in the metagenome of the community that encode the degradation pathways of a range of substrates: aldehydes, octane, nylon-6 oligomers, and cyclitols. These compounds, as well as the related molecules, are often detected in municipal wastewater as organic pollutants, mainly in industrial wastewater [67]. Similarly, incubation with drugs reduced the representation of genes encoding the metabolic pathways of mineral macronutrients by 2 orders of magnitude, such as microbial sulfur oxidation, nitrification, denitrification, and the degradation of methylphosphonate. It is expected that such changes will reduce the potential of a community regarding its ability to remove macronutrients from wastewater.

At the same time, incubation of communities in the presence of drugs and high concentrations of bioavailable nitrogen and phosphorus increased the representation of pathways involved in catabolism and the biosynthesis of nucleotides and nucleosides in their metagenome by 2 orders of magnitude. Apparently, the potential of ABC components to involve inorganic nitrogen and phosphorus in metabolism remains partially. For amino acids, carbohydrates, and biopolymers, the representation of catabolism genes increased to a greater extent as compared to biosynthesis genes.

The studied drugs had different effects on certain metabolic pathways in the community metagenome. Thus, the relative representation of pathways associated with resistance to CTA increased four orders of magnitude (by the mechanism of the repair of cell-wall defects, since CTA interferes with the synthesis of cell-wall components) [68]. In addition, CTA in contrast to DF reduced the representation of siderophore biosynthesis pathways by an order of magnitude, which may be an indirect indicator of microalgal proliferation in ABC samples incubated with the antibiotic.

In order to clarify the potential functional profile of ABC samples from the Zvenigorod wastewater-treatment plants, markers of certain metabolic pathways were sought for in raw long reads obtained by nanopore sequencing. We used the algorithms of BugSeq classifier, which was originally developed to search for markers of antibiotic resistance in microbial communities, to detect relevant genes in the studied ABC samples. The ABC samples incubated with the addition of only macronutrients possessed the *arr* rifamycin-resistance gene involved in ADP-ribosylation [69]. The *bla* family genes encoding enzymes from the family of β-lactamases capable of inactivating β-lactam antibiotics and nonspecific for CTA were found in samples incubated with CTA [70]. Representatives of the *Brevundimonas* and *Sphingopyxis* genera are carriers of the *bla* family genes as well. It is noted that in the sample incubated with DF and macronutrients, copies of the *bla* family genes were found, as well as of the *mph*(*F*) gene involved in the development of resistance to macrolide-group antibiotics, including azithromycin, erythromycin, and clarithromycin [69]. Therefore, under the influence of drugs entering wastewater, microorganisms from wastewater-treatment-plant communities may develop nonspecific and cross-(multiple) drug resistance, including to antibiotics.

## CONCLUSIONS

The effect of medicinal substances on the morphophysiological properties and metagenomes of ABCs from water-treatment plants consisting of microalgae and/or cyanobacteria has been studied. The metagenomic results obtained using 16S rRNA amplicon short-read sequencing and long-read metagenomics sequencing of the complete community metagenome were compared, as well as traditional methods of the morphophysiological monitoring of ABCs were used.

It was shown that incubation of the ABCs for 31 days with drugs causes enrichment of the ABCs with antibiotic-resistant bacteria. Despite the fact that the rate of phosphorus removal was retained, the genetically determined potential of the community in terms of its ability to remove nutrients tended to decrease. In parallel, cyanobacteria originally present in the community were replaced with eukaryotic microalgae.

Despite the significant amount of data on changes in the metabolism of the studied ABCs obtained using the PICRUSt2 algorithm, they do not allow us to unambiguously judge the direction of changes in the metabolic potential of the communities. The reason is the limited accuracy of microorganism identification using the DNA metabarcoding method on NGS platforms, the results of which are used by the PICRUSt2 algorithm.

In contrast, the analysis of raw long reads (using BugSeq algorithms) revealed that the representation of antibiotic-resistance markers increased in ABCs incubated with antibiotic. It is noted that there was an increase in the representation of resistance genes to other types of antibiotics that were not used in this work. Thus, the study confirms the fundamental possibility of the gradual formation of nonspecific and/or cross-(multiple) drug resistance, including to antibi-

otics, in microorganisms from wastewater-treatment-plant communities under the action of drugs entering municipal wastewater. The results also indicate that metagenomic sequencing is a more convenient, accurate, and informative method for monitoring of microbial communities.

## ACKNOWLEDGMENTS

We are grateful to OOO Zvenigorodsky Vodokanal Municipal Water Supply Service for the opportunity to take samples. The photosynthetic activity was measured using equipment from the Shared Use Center "Phenotyping of Phototrophic Microorganisms" of Moscow State University. NGS-metabarcoding studies were carried out using equipment of the Shared Use Center "Genomic Technologies, Proteomics and Cell Biology" of the All-Russian Research Institute of Agricultural Microbiology.

## FUNDING

This study was supported by the Scientific and Educational School of Moscow State University "Molecular Technologies of Living Systems and Synthetic Biology" (project no. 004053, nanopore sequencing) and the Russian Science Foundation (grant no. 21-74-20004, other research).

## ETHICS APPROVAL AND CONSENT TO PARTICIPATE

This work does not contain any studies involving human and animal subjects.

## CONFLICT OF INTEREST

The authors of this work declare that they have no conflicts of interest.

## REFERENCES

1. M. J. Gallardo-Altamirano, P. Maza-Márquez, N. Montemurro, et al., Chemosphere **233**, 828 (2019). https://doi.org/10.1016/j.chemosphere.2019.06.017
2. Y. X. Gao, X. Li, X. Y. Fan, et al., Bioresour. Technol. **351**, 127016 (2022). https://doi.org/10.1016/j.biortech.2022.127016
3. B. Ji and Y. Liu, ACS ES&T Water **1**, 2459 (2021). https://doi.org/10.1021/acsestwater.1c00303
4. C. A. Sepúlveda-Muñoz, I. de Godos, and R. Muñoz, Symmetry **15**, 525 (2023). https://doi.org/10.3390/sym15020525
5. S. Kathi, S. Singh, R. Yadav, et al., Front. Chem. Eng. **5**, 1129783 (2023). https://doi.org/10.3389/fceng.2023.1129783
6. F. G. Magro, J. F. Freitag, A. Bergoli, et al., Rev. Environ. Sci. Biotechnol. **20**, 865 (2021). https://doi.org/10.1007/s11157-021-09587-9
7. C. Wang, L. Jiang, Y. Zhang, et al., Environ. Sci. Pollut. Res. **30**, 95975 (2023). https://doi.org/10.1007/s11356-023-29147-8
8. I. Eheneden, R. Wang, and J. Zhao, Sci. Total Environ. **891**, 164489 (2023). https://doi.org/10.1016/j.scitotenv.2023.164489
9. F. Marchetto, M. Roverso, D. Righetti, et al., Life **11**, 1300 (2021). https://doi.org/10.3390/life11121300
10. E. Clagnan, M. Dell'Orto, K. Štěrbová, et al., Bioresour. Technol. **374**, 128781 (2023). https://doi.org/10.1016/j.biortech.2023.128781
11. L. Qixin, F. Xuan, S. Zhiya, et al., Bioresour. Technol. **354**, 127161 (2022). https://doi.org/10.1016/j.biortech.2022.127161
12. K. Iqbal, A. Saxena, P. Pande, et al., Bioresour. Technol. **354**, 127203 (2022). https://doi.org/10.1016/j.biortech.2022.127203
13. P. Shetty, I. Z. Boboescu, B. Pap, et al., Front. Energy Res. **7**, 52 (2019). https://doi.org/10.3389/fenrg.2019.00052
14. W. H. Leong, K. Kiatkittipong, W. Kiatkittipong, et al., Processes **8**, 1427 (2020). https://doi.org/10.3390/pr8111427
15. J. Chen, X. Liu, T. Lu, et al., Water Res. **252**, 121214 (2024). https://doi.org/10.1016/j.watres.2024.121214
16. L. Tang, M. Gao, S. Liang, et al., Water Res. **253**, 121315 (2024). https://doi.org/10.1016/j.watres.2024.121315
17. A. Saravanan, P. S. Kumar, S. Varjani, et al., Chemosphere **271**, 129540 (2021). https://doi.org/10.1016/j.chemosphere.2021.129540
18. V. K. Patel, N. K. Sahoo, A. K. Patel, et al., *Algal Biofuels: Recent Advances and Future Prospects*, Ed. By Gupta S. (Springer Int., Cham, 2017), p. 109. https://doi.org/10.1007/978-3-319-51010-1_6
19. G. Padmaperuma, R. V. Kapoore, D. J. Gilmour, et al., Crit. Rev. Biotechnol. **38**, 690 (2018). https://doi.org/10.1080/07388551.2017.1390728
20. D. Nagarajan, D.-J. Lee, S. Varjani, et al., Sci. Total Environ. **845**, 157110 (2022). https://doi.org/10.1016/j.scitotenv.2022.157110
21. L. Zhang, F. Chen, Z. Zeng, et al., Front. Microbiol. **12**, 766364 (2021). https://doi.org/10.3389/fmicb.2021.766364
22. T. W. Lane, P. D. Lane, C. Y. Koh, et al., *Pond Crash Forensics: Microbiome Analysis and Field Diagnostics* (No. SAND2013–6673C) (2013).
23. B. P. Thomma, M. F. Seidl, X. Shi-Kunne, et al., Fungal Genet. Biol. **90**, 24 (2016). https://doi.org/10.1016/j.fgb.2015.08.010
24. G. M. Douglas, V. J. Maffei, J. R. Zaneveld, et al., Nat. Biotechnol. **38**, 685 (2020). https://doi.org/10.1038/s41587-020-0548-6
25. F. Wemheuer, J. A. Taylor, R. Daniel, et al., Environ. Microbiol. **15**, 11 (2020). https://doi.org/10.1186/s40793-020-00358-7

26. A. K. Berkovich, O. A. Pyshkina, A. A. Zorina, et al., Biochemistry Moscow **89** (Suppl. 1), S234–S248 (2024). https://doi.org/10.1134/S000629792414013X

27. A. Edwards, A. Debbonaire, S. Nicholls, et al., BioRxiv, 073965 (2016). https://doi.org/10.1101/073965

28. M. Jain, S. Koren, K. H. Miga, et al., Nat. Biotechnol. **36**, 338 (2018). https://doi.org/10.1038/nbt.4060

29. F. J. Rang, W. P. Kloosterman, and J. de Ridder, Genome Biol. **19**, 90 (2018). https://doi.org/10.1186/s13059-018-1462-9

30. J. Parker, A. J. Helmstetter, D. Devey, et al., Sci. Rep. **7**, 8345. https://doi.org/10.1038/s41598-017-08461-5

31. A. Belcour, C. Frioux, M. Aite, et al., eLife **9**, e61968 (2020). https://doi.org/10.7554/eLife.61968

32. F. Zorrilla, F. Buric, K. R. Patil, et al., Nucleic Acid Res. **49**, e126 (2021). https://doi.org/10.1093/nar/gkab815

33. D. K. Kuppa Baskaran, S. Umale, Z. Zhou, et al., ISME Commun. **3**, 42 (2023). https://doi.org/10.1038/s43705-023-00242-8

34. W. Inskeep, Z. Jay, M. Herrgard, et al., Front. Microbiol. **4**, 95 (2013). https://doi.org/10.3389/fmicb.2013.00095

35. K. R. Patil and A. C. McHardy, Genome Biol. Evol. **5**, 1470 (2013). https://doi.org/10.1093/gbe/evt105

36. D. H. Huson, A. F. Auch, J. Qi, et al., Genome Res. **17**, 377 (2007). https://doi.org/10.1101/gr.5969107

37. V. Mallawaarachchi, A. Wickramarachchi, and Y. Lin, Bioinformatics **36**, 3307 (2020). https://doi.org/10.1093/bioinformatics/btaa180

38. A. Blanco-Míguez, F. Beghini, F. Cumbo, et al., Nat. Biotechnol. **41**, 1633–1644 (2023). https://doi.org/10.1038/s41587-023-01688-w

39. M. Karlicki, S. Antonowicz, and A. Karnkowska, Bioinformatics **38**, 344 (2021). https://doi.org/10.1093/bioinformatics/btab672

40. W. Y. Chia, TangD. Y. Ying, K. S. Khoo, et al., Environ. Sci. Ecotechnol. **4**, 100065 (2020). https://doi.org/10.1016/j.ese.2020.100065

41. A. K. Priya, A. A. Jalil, S. Vadivel, et al., Chemosphere **305**, 135375 (2022). https://doi.org/10.1016/j.chemosphere.2022.135375

42. S. G. Vasilyev, P. A. Zaitsev, O. I. Baulina, et al., Ross. Nanotekhnol. **18**, 53 (2023). https://doi.org/10.56304/S1992722323010168

43. X. Cheng, J. Xu, G. Smith, et al., Environ. Manage. **295**, 113129 (2021). https://doi.org/10.1016/j.jenvman.2021.113129

44. J. O. Ovis-Sánchez, V. D. Perera-Pérez, G. Buitrón, et al., Sci. Total Environ. **882**, 163545 (2023). https://doi.org/10.1016/j.scitotenv.2023.163545

45. S. Vasilieva, A. Lukyanov, C. Antipova, et al., Int. J. Mol. Sci. **24**, 1310988 (2023). https://doi.org/10.3390/ijms241310988

46. G. M. Vingiani, P. De Luca, A. Ianora, et al., Mar. Drugs **17**, 459 (2019). https://doi.org/10.3390/md17080459

47. D. M. Portik, C. T. Brown, and N. T. Pierce-Ward, BMC Bioinformatics **23**, 541 (2022). https://doi.org/10.1186/s12859-022-05103-0

48. L. Richardson, B. Allen, G. Baldi, et al., Nucleic Acids Res. **51**, D753 (2022). https://doi.org/10.1093/nar/gkac1080

49. S. Ota and S. Kawano, Bio-protocol **7**, No. 17 (2017). https://doi.org/10.21769/bioprotoc.2539

50. S. T. Bates, D. Berg-Lyons, J. G. Caporaso, et al., ISME J. **5**, 908 (2010). https://doi.org/10.1038/ismej.2010.171

51. A. M. Bolger, M. Lohse, and B. Usadel, Bioinformatics **30**, 2114 (2014). https://doi.org/10.1093/bioinformatics/btu170

52. P. J. McMurdie and S. Holmes, PLoS One **8**, e61217 (2013). https://doi.org/10.1371/journal.pone.0061217

53. E. S. Wright, R J. **8**, 352 (2016).

54. J. G. Caporaso, J. Kuczynski, J. Stombaugh, et al., Nat. Methods **7**, 335 (2010). https://doi.org/10.1038/nmeth.f.303

55. P. Yilmaz, L. W. Parfrey, P. Yarza, et al., Nucleic Acids Res. **42**, D643 (2014). https://doi.org/10.1093/nar/gkt1209

56. H. S. Horn, Am. Natur. **100**, 419 (1966).

57. R. M. Schuurmans, P. van Alphen, J. M. Schuurmans, et al., PloS One **10**, e0139061 (2015). https://doi.org/10.1371/journal.pone.0139061

58. A. E. Solovchenko, S. G. Vasilieva, P. A. Zaitsev, et al., J. Appl. Phycol. **34**, 1 (2022). https://doi.org/10.1007/s10811-021-02660-4

59. D. S. Sánchez-Sandoval, O. González-Ortega, J. Vazquez-Martínez, et al., 3 Biotec **12**, 210 (2022). https://doi.org/10.1007/s13205-022-03268-2

60. E. Dias, M. Oliveira, D. Jones-Dias, et al., Front. Microbiol. **6**, 799 (2015). https://doi.org/10.3389/fmicb.2015.00799

61. A. E. Solovchenko, T. T. Ismagulova, A. A. Lukyanov, et al., J. Appl. Phycol. **31**, 2755 (2019). https://doi.org/10.1007/s10811-019-01831-8

62. M. Henderson, S. J. Ergas, K. Ghebremichael, et al., Water **14**, 758 (2022). https://doi.org/10.3390/w14050758

63. J. Singh and I. S. Thakur, Algal Res. **11**, 294 (2015). https://doi.org/10.1016/j.algal.2015.07.010

64. L. N. N. Shipingana, H. P. Shivaraju, and S. R. Yashas, Appl. Water Sci. **12**, 16 (2022). https://doi.org/10.1007/s13201-022-01570-1

65. J. Y. Lee, I. R. Monk, A. Gonçalves da Silva, et al. Nat. Microbiol. **3**, 1175 (2018). https://doi.org/10.1038/s41564-018-0230-7

66. R. Caspi, R. Billington, I. M. Keseler, et al., Nucleic Acids Res. **48**, D445 (2020). https://doi.org/10.1093/nar/gkz862

67. H. B. Ahmed, M. H. Helal, M. H. Abdo, et al., Polym. Test. **104**, 107381 (2021). https://doi.org/10.1016/j.polymertesting.2021.107381

68. J. W. Johnson, J. F. Fisher, and S. Mobashery, Ann. New York Acad. Sci. **1277**, 54 (2013). https://doi.org/10.1111/j.1749-6632.2012.06813.x

69. D. A. Rowe-Magnus and D. Mazel, Curr. Opin. Microbiol. **2**, 483 (1999). https://doi.org/10.1016/s1369-5274(99)00004-1

70. S. Pournaras, A. Tsakris, M. Maniati, et al., J. Antimicrob. Chemother. **46**, 4026 (2002). https://doi.org/10.1128%2FAAC.46.12.4026-4028.2002

*Translated by M. Novikova*